WHAT IF…? COMPUTATIONAL ANATOMY IN THE GRANULAR LAYER OF THE CEREBELLAR CORTEX

Mike Gilbert[a] (corresponding author), Anders Rasmussen[b]

[a]School of Psychology, College of Life and Environmental Sciences, University of Birmingham B15 2TT, UK

ORCID: 0000-0003-4415-6915

[b]Department of Experimental Medical Science, Lund University, BMC F10, 22184 Lund, Sweden

ORCID: 0000-0003-4477-369X

Correspondence: m.gilbert.1@bham.ac.uk

ABSTRACT/SUMMARY

Neuronal firing rates code values which the brain computes. It is thought that, at a collective level, information is represented in high resolution which is replicable with computer-like high fidelity and allows computations to be powerful. We challenge that in the cerebellum. We find plausibly that there is a computational effect, unaided and unlearned, of the combination of anatomy and the idea that the cerebellum is the physical form of a computational network of linear units. A unit can be a cell, part of a cell or some other structure. Units randomly sample afferent data. Anatomy mimics random sampling of the whole afferent layer of firing rates, with replacement, notwithstanding that a single unit receives unchanging contact from a tiny fraction of cells in the afferent layer. Cell morphologies and network geometry are explicable as bespoke adaptations for this function. Input data are converted to a (very) low-resolution, coarsely-pixellated internal picture. This is functional. It provides an otherwise elusive mechanism to orchestrate firing of large cell groups – microzones – downstream, and it solves the problem of working blind with unreliable information.

Keywords: cerebellum; theory; hypothesis; model; computational anatomy; cerebellar cortex; granular layer; network; input layer; code

1. Introduction

It is generally assumed that the representation of information in the brain is in high resolution and replicable with high fidelity, and that those features make it precise and characterise the inputs to sophisticated computations. Replicability is an important assumption of neural network learning models, including cerebellar models. We challenge these ideas by making a case in evidence and *in silico* that the cerebellum converts input signals into a pixellated, very low-resolution internal code. This is done by the unaided, passive computational effect of anatomy and linear transmission. The internal code does not need to have a replicable physical form. This allows the cerebellum to process input data blind below a scale threshold, working with unreliable data, and coordinate firing of large cell groups downstream.

There is now a substantial body of evidence that rate-coded information is linearly conserved in communication between cerebellar neurons [1-8], and that cells are adapted for faithful transmission [9-15]. Firing rates that linearly code behavioural and task metrics have been observed 'at all levels of the cerebellar circuit' [16 p.239, citing 30 sources]. Evidence of linear signalling in the granular layer is rich. We include a review in the Methods section to which we cross refer from the main text.

The inner layer of the cerebellar cortex, the granular layer, receives the main excitatory input to the cerebellum, from mossy fibres. Mossy fibres contact both granule cells and large inhibitory interneurons, Golgi cells. Golgi cells in turn inhibit granule cells. The granule cell axon rises into the outer layer, the molecular layer, where it divides in two to form parallel fibres, which lie parallel to the cerebellar surface and other parallel fibres. Parallel fibres make contact in passing on Purkinje cells, which carry the sole output of the cerebellar cortex.

In the traditional learning model, the function of the granular layer is to generate patterns of active and inactive parallel fibres that are repeated if the cerebellum receives the same mossy fibre input. Following training, the response of Purkinje cells to parallel fibre firing rates is displaced by the compound effect of learned changes of synaptic transmission strengths. Replicability of patterns is important (and assumed) so that signals are received by the correct set of modified synapses. Learned changes of synaptic weights are also a core feature of artificial neural network learning models.

However, it is not clear that input to the cerebellum is ever replicated. Around 4,000 mossy fibres innervate the region that supplies parallel fibre input to a single Purkinje cell. It may not be a safe assumption that conditions upstream are routinely repeated with precision sufficient to consistently (or perhaps ever) generate a repeat of the same inputs. A second issue is that single neurons and synapses are not reliably consistent performers. Neurons even of the same type are by no means replicas, and

synaptic transmission involves random variables. Evidence of linear transmission is also problematic for models that use synaptic weight changes. It is not inconceivable they could be reconciled, but it feels forced since it is the function of learning to *displace* a rate-coded response.

Neuron-to-neuron transmission involves the complex interaction of a large array of often co-dependent biophysical and other variables which are specific to the cell types making and receiving contact. Part of the significance of evidence of linearity is that despite the seeming clamour, linear relationships are in fact conserved. There are a number of examples that the cerebellum is adapted to disengage or otherwise compensate for intrinsic non-linear properties of neurons and synapses [13, 14, 17, 18]. This is – plausibly, we submit – part of a general strategy of isolating the effect of parameters that code information and controlling for other variables. In this view, the cerebellum is a physical implementation of networked linear units. A unit can be a cell, part of a cell or some other structure. Units sample afferent data. Signalling by a layer of units at any given instant in time is the physiological form of a data set. Anatomy mimics random sampling of the whole afferent layer of firing rates, with replacement, notwithstanding that a single unit receives unchanging contact from a tiny fraction of cells in the afferent layer. Cell morphologies and network geometry are explicable as bespoke adaptations for this function. In this contention, neuronal sums are not complex but have a statistical effect at collective level which is exploited to code information. Sampling units provide model parameters. We field evidence in the main

text to explain the derivation of model parameters. Parameter values are supplied by the literature. Our main findings are listed in the Discussion section. We include a statement of the relevant parts of the hypothesis at or near the beginning of each section.

2. Mossy fibres

2.1 Anatomy, 'ranks' and 'files'

Mossy fibres give rise to sagittally-extending collaterals, the direction of the long axis of microzones (Fig 1). These in turn give rise to multiple distal branches, each ending in a cluster of terminals [19-22]. Terminal clusters are sagittally aligned and separated by a randomly variable distance typically not less than 200 µm [19, 20] measured from edge to edge of clusters (so they are separated by a greater distance measured from centre to centre). Terminals themselves are intimately and randomly intermingled with terminals of other mossy fibres.

Accordingly, mossy fibres do not terminate at a point but a region with dimensions: the field occupied by a terminal cluster. A single mossy fibre gives rise to several terminal branches and each of those to several terminals, such that a sagittal strip of the granular layer receives multiple copies of every signal at each of multiple locations.

Cluster size is variable (because it depends on the number of terminals and how tightly clustered they are), averaging 200 µm sagittally x 150 µm mediolaterally [20]. We term the average dimensions of a cluster a 'field'. The granular layer is anatomically seamless. A field is simply a nominal division that we use for modelling. A sagittal row of 75–100 fields laid end to end has the area (viewed from the cerebellar surface) of a mid-range microzone [23-26]. We term a row of fields a 'rank'. Ranks are functionally but not anatomically discrete.

Each terminal is ensheathed by a semi-permeable membrane which restricts neurotransmitter diffusion, a structure taken together termed a glomerulus. Excitation of granule cells and Golgi cells by mossy fibres, and inhibition of granule cells by Golgi cells, all take place here.

Figure 1

2.2 Hypothesis

Mossy fibre anatomy is an anatomical solution to a computational problem. The cerebellum exploits statistical effects of random sampling called the central limit theorem. For the effects to occur, samples must be independent, also termed sampling 'with replacement' (in the illustration sometimes used, coloured balls selected at random from a bag are put back in the bag between samplings). Clearly, physical replacement is impossible because neither a terminal cluster nor a terminal can be in

more than one place at the same time. However, anatomy simulates replacement. The distributed probabilities of the number of terminal branches per mossy fibre are the same as the probabilities of the number of repeat samplings if rates received by a rank were in fact independently randomly sampled by fields. Similarly, the distributed probabilities of the number of terminals per cluster are the same as the distributed probabilities of the number of repeat samplings if rates received by a field were in fact randomly sampled with replacement by individual target neurons. Note that it is the population of *rates* that are hypothetically sampled with replacement, and not *signals.* The population of signals includes copies of rates because of branching and clustering. Copies are an anatomical device to mimic sampling rates with replacement.

2.3 Terminal branching simulates sampling with replacement

If each mossy fibre could terminate in only one field, a mossy fibre 'sampled' by one field clearly cannot also be sampled by any others. Termination by a single mossy fibre in a random number of terminal branches, at multiple locations, removes that restriction.

In theory, sampling with replacement should mean any number of fields can receive the same signal, up to all of them. Clearly this is not true – there is still an anatomical limit. But in practice even with real replacement the number of repeat samplings is constrained by a probability distribution. If, then, the number of terminal branches per

mossy fibre has the same probability distribution, branching has the same result as if firing rates received by each field in a rank were in fact a random sample with replacement of firing rates received by the rank as a whole.

We can test that by calculating the probability distribution in the hypothetical case that mossy fibres did not branch terminally and rates were in fact sampled with replacement. The probability, p, that a given rate is selected k times in taking N samples, sample size x, assuming mossy fibres each give rise to an average of m terminal branches, is given by

$$\left[{Nx!}/{k!\,(Nx-k)!}\right] * \left[{1}/{(Nx/m)}\right]^{k} * \left[1-\left({1}/{(Nx/m)}\right)\right]^{Nx-k}$$

The results are shown in Table 1.

Table 1. Probability p of k repeat selections of a single mossy fibre

k	0	1	2	3	4	5	6	7	8	9	10	11
p	0.007	0.034	0.084	0.140	0.175	0.175	0.146	0.104	0.065	0.036	0.018	0.008

Although data are scarce, the number of repeat selections is consistent with what we know about the biological range of the number of terminal clusters per mossy fibre [20, 27]. Estimated by this method, the mean is 4–5.

2.4 Terminal clusters simulate sampling with replacement

The principle is the same here but at local, field scale. Mossy fibre terminal clustering, and random intermingling with terminals of other mossy fibres (Fig 1), means that contact on any particular cell does not mean the same mossy fibre cannot also contact cells somewhere else. Again, to approximate independence, it is only necessary for the number of repeat selections of a signal to have the same probability distribution as if there was actual replacement.

A practical problem with the strategy of clustering is that a target could receive the same signal twice (or more). The risk is mitigated by taking small samples. A sample size of 4 is small enough for a low risk. Granule cells average 4 dendrites, each receiving contact from a single terminal, and we estimate that Golgi cells receive an average of 4 inputs to each of their basal dendrites (see derivation of parameters in the next section). Given m x 100 terminals and an independent and equal chance that contact is by any terminal, the probability of an nth contact by the same mossy fibre on a single dendrite is:

$$P_n = \left[\prod_{x=2}^{n}\left(\frac{m-x+1}{100m-x+1}\right)\right] \times \frac{y!}{x!\,(y-x)!}$$

where y is the number of inputs to a single dendrite and m is the number of terminals per cluster, provided by (for illustration) 100 mossy fibres. Calculated in this way,

around one in every twenty samples contains a duplicate, and less than two in a thousand contain more than one. The actual fractions are smaller because the number of mossy fibres that innervate a field is higher, around 180 (see Methods, Derivation of mossy fibre rates).

Quasi-sampling by each field of mossy fibre firing rates received as input to the rank as a whole, and by cells in each field of rates received by that field, is a biological facsimile of simultaneous random sampling with replacement by single neurons of input rates to a whole rank.

3. **Golgi cells**

3.1 Hypothesis

Despite forming an anatomically seamless dense mesh of axonal filaments that fills the granular layer, Golgi cells work in groups: ensembles. An ensemble is the population of a sagittal row of three fields. Groups are not anatomically bounded or even functionally discrete, but function as a single unit for the anatomical reason that the axonal range of all Golgi cells in a 3-field row includes all or most of the middle field. Put another way, each field defines a functional population of Golgi cells – an ensemble – being those cells with convergent input to that field. Ensembles perform a

computational conversion of mossy fibre rates into inhibition of granule cells. The computation is (chiefly) a statistical result of random sampling, in two steps. At the first step, Golgi cell basal dendrites receive contact from a random sample of mossy fibres that innervate a field (strictly speaking, they randomly sample terminals); and in the second step, middle-field glomeruli each receive innervation by a random sample of Golgi cells. The effect of the computation is to synchronise inhibition of granule cells in the middle field. The strength of inhibition is linearly related to the mean of mossy fibre firing rates received as input to the entire rank.

Ensembles conflate sagittally anatomically and functionally. Ensembles in a sagittal strip all return the same output (because they all perform the same computation on input data with the same frequency distribution). Effectively: the Golgi cell population of a whole rank functions as a single unit.

3.2 The Golgi cell computation

Say a population of values (with any frequency distribution) is randomly sampled. There are n samples, sample size m. If we take the mean (or sum) of each sample, and n is large, the sample means have a normal or near-normal distribution, by the central limit theorem. (This works even if m is a range.) The new distribution is centred on the same mean as the sampled distribution, but narrower. Modest values of n or m give an

217 untidy result. However, if the new distribution is then itself randomly sampled, and the
218 process is repeated, the results get tidier and narrower.

219 We envisage that in motor circuits during behaviour signalling is analogue, avoiding the
220 noise caused by discrete signals. So, for example, Golgi cell dendritic signalling is a
221 sustained state under modulation by fluctuating mossy fibre rates. Similarly, GABA
222 spillover into the intraglomerular space, almost exclusively the agent of granule cell
223 inhibition, becomes elevated by a build-up during behaviour, so that this too is at a
224 sustained level, controlled by afferent Golgi cell rates. Thus, at each step, data are
225 coded at any moment in a snapshot of a state of change.

226 We tested the hypothesis *in silico* by simulating a rank. Derivation of model
227 parameters is described in: Methods, Derivation of ensemble dimensions and model
228 parameters. Mossy fibre rates sampled by Golgi cells in each field were obtained by
229 sampling from a distribution representing signals received as input to the rank as a
230 whole, which were randomly generated subject to constraints on the shape of the
231 distribution. This was modified to take into account mossy fibre terminal branching
232 and clustering, random variation of the number of terminals per cluster and clusters
233 per cell, and the fact that most clusters fall partly inside and partly outside a field (see
234 Methods, Derivation of mossy fibre rates).

235 This gave the number of mossy fibre signals, firing rates and the number of copies of
236 each rate received by each field, and therefore input to an ensemble territory,

237 populated by 30 Golgi cells, 10 per field. There are ~700 mossy fibre terminals per
238 field. As far as we know (and we propose), contact by mossy fibres on Golgi cells is at
239 random at field scale, i.e., inputs to a single basal dendrite are provided by a random
240 sample of local terminals. The number of physiological samplings is equal to the
241 number of basal dendrites per field; sample size is the number of mossy fibres which
242 make contact on each dendrite. The effect is sustained dendritic depolarisation under
243 modulation by a linear function of input rates (see Methods, Linear transmission of
244 mossy fibres to Golgi cells), which we take as the mean.

245 Taking the sample means generates a new set of values (Fig 2 column 2) with a smaller
246 range and centred on the mean, which is linearly related to the mean of the sampled
247 distribution. Basal dendritic charge transfer is passive and little filtered [11, 28].
248 Integration of dendritic states at the Golgi soma is represented by taking the mean of
249 dendritic charge, for each simulated cell. Golgi cell firing rates have a linear
250 relationship with the amplitude of depolarising current [29], suggesting (and we
251 assume) a linear conversion of somatic membrane potential into the Golgi cell firing
252 rate.

253 The output is a third data set, Golgi cell firing rates (Fig 2 column 3), on the same
254 normalised scale. Each glomerulus in the middle field receives innervation from a
255 random subset of Golgi cells afferent to the field, and accordingly independently
256 randomly samples Golgi cell firing rates. Golgi cells inhibit granule cells in the

257 glomerulus. A granule cell extends a single dendrite into a glomerulus, typically
258 receiving synaptic contact from two or three Golgi cells [30]. However, inhibition of
259 granule cells by Golgi cells is almost entirely by GABA spillover into the intraglomerular
260 space [5], via extrasynaptic receptors [31, 32] (see Methods, Linear transmission of
261 Golgi cells to granule cells). This effectively increases the Golgi cell to granule
262 convergence ratio, since the number of Golgi cells that are functionally afferent to a
263 granule cell is not the number that make direct contact, but the number afferent to a
264 glomerulus. The membrane around a glomerulus restricts GABA diffusion so that
265 signalling is by modulation of the intraglomerular concentration of GABA, which in turn
266 reflects the rate it is released. The rate it is released by a single cell is proportional to
267 the firing rate of that cell. The sum of rates is proportional to the mean. The
268 convergence ratio is sample size; the number of samples is the number of glomeruli
269 per field (~700, the same as terminals). Intraglomerular GABA concentration is under
270 continuous modulation at a sustained level which we took to be a linear function of
271 the mean of afferent Golgi cell rates, given by the sample means. The number of Golgi
272 cells afferent to a glomerulus is unreported, as far as we know. We take it as a random
273 number in the range 8–12, generated for each glomerulus. We tested other ratios to
274 confirm that the ratio does not affect the ensemble computation (Supplementary
275 Materials).

276 This generates a final population of values (Fig 2 columns 4 and 5), the output of the
277 ensemble conversion. There are 700 outputs, representing glomeruli in the middle

field. All granule cells that extend a dendrite into the same glomerulus receive equal inhibition (of that dendrite).

3.3 Results

3.3.1 An ensemble

There is a progressive narrowing of the data range at each step. Inputs to the system are converted to narrowly-grouped and normally-distributed outputs. The narrow output range indicates that inhibition is locally synchronised, i.e., granule cells in a field receive co-modulated inhibition. Inhibition has a linear relationship with mossy fibre rates, acting through the ensemble conversion. These results are independent of the shape of mossy fibre rates.

Figure 2

3.3.2 A rank

We next used the ensemble conversion to derive inhibition of granule cells in a sagittal row of 100 fields, a rank. The results are shown in Figure 3. As ensembles all perform the same computation and take as input (at any moment) the same frequency distribution of input rates, or nearly the same distribution, they all return the same output, or nearly the same output. There are 700 outputs per field. The mean of outputs, taken for each field, has a narrow range centred on the mean of mossy fibre

input rates to the whole rank. Field-to-field variation of output appears to be inherent in the mechanism – i.e., caused by uncertainty of the outcome of random sampling – so it has a predictable range which the system can be built to tolerate.

Conclusion: Golgi cells in a rank act as a single functional unit. Ensembles conflate in the sagittal direction functionally as they do anatomically. As a result, the whole granule cell population *of a rank* receive synchronised inhibition which is linearly related to the mean of mossy fibre rates.

Figure 3

4. Granule cells

4.1 The fraction of active granule cells is reliably regulated by feed-forward inhibition at low density

4.1.1 Hypothesis

Anatomy simulates independent random sampling by a single granule cell of the population of mossy fibre input rates to the whole rank (section 2). There is a competition for influence between mossy fibre excitation and Golgi cell inhibition of granule cells. The competition takes place in the glomerulus. During behaviour, this takes place ceaselessly. The strength of inhibition is synchronised between glomeruli

313 that populate a rank (section 3), so that all mossy fibre signals compete, at any
314 moment, against the same inhibitory threshold. The outcome in each glomerulus is
315 independent of the outcome at other terminals, including other terminals that
316 innervate the same granule cell. To fire, a granule cell must receive a minimum
317 number of mossy fibre inputs that prevail in the glomerular competition. The
318 probability that enough prevail depends, at any moment, on the strength of inhibition.
319 Since inhibition is synchronised, the probability is the same for all granule cells at any
320 time. The number that fire is very near the expected proportion (the number predicted
321 by probability) because granule cells are numerous. Inhibition has a linear relationship
322 with mossy fibre firing rates (section 3). This is always conserved (by the Golgi cell
323 ensemble conversion) regardless of the mossy fibre distribution (section 3). So, the
324 probability is invariant, and therefore so is the proportion of active granule cells.

325 Note: the idea of an all-or-nothing result of the intraglomerular 'balance' of excitation
326 and inhibition has appeared previously [33].

327 4.1.2 Anatomy

328 Granule cells receive input to each dendrite from a single mossy fibre. Granule cells
329 have 3–5 dendrites, averaging 4 (the simulation assumes 4, but the result is the same
330 with 3–5). Each dendrite of a single granule cell extends into a different glomerulus.
331 Estimates vary of the number of granule cells that receive contact from a single mossy
332 fibre terminal. 50 is mid-range [34, 35], but estimates vary significantly [2]. 50 is

333 consistent with our estimates of the number of terminals and granule cells in a field.
334 The granule cell sampling unit is the whole cell since it receives only a single input rate
335 to each dendrite. Sample size is therefore 4, and the number of samples per field is the
336 number of granule cells, which we estimate at 8,750 (see Methods, Derivation of
337 mossy fibre rates).

338 4.1.3 Feed-forward inhibition regulates the probability that granule cells 339 fire

340 Excitation and inhibition compete for influence in a glomerulus. It is unclear if there is
341 always an emphatic winner, but a swing in the dominant direction may be amplified by
342 positive feedback, acting through presynaptic receptors. Activation of presynaptic
343 $GABA_B$ receptors on mossy fibres inhibits glutamate release [36], while activation of
344 presynaptic mGluR2 receptors on Golgi cells inhibits GABA release [37]. We postulate
345 that only mossy fibre signals which prevail in the glomerular competition contribute
346 significantly to granule cell depolarisation. To fire, a granule cell must receive a
347 minimum number of competitive mossy fibre signals – thought to be three [38, 39].
348 Certainly, one is too few [5, 40, 41].

349 The probability that a given granule cell receives three competitive signals and
350 therefore fires is a function of the percentage of mossy fibre signals that are
351 competitive. The expected number of granule cells that fire in a field is given by

$$E_{fld} = T \sum_{x=j}^{n} \left[\frac{n!}{(n-x)!x!} [P(e > i)]^{x} [1 - P(e > i)]^{n-x} \right]$$

where T is the total number of granule cells per field, n is the number of dendrites per granule cell, and j is the minimum number of dendrites that must receive dominant excitation, $e > i$. The proportion of granule cells that fire is near the expected number by the law of large numbers. The percentage of mossy fibre signals that are competitive is always the same because inhibition scales with the mean of mossy fibre rates (because Golgi cells translate mossy fibre firing rates into proportional inhibition). As the percentage is unvarying, so is the probability.

Probability is an abstraction with no direct physiological counterpart. The simulation does not include a binomial function but derives output from input by comparing excitatory to inhibitory input to each glomerulus, the way we claim it is derived physiologically. The equation is simply shorthand – biology exploits chance and large numbers to generate the same result (as if inputs were passed through the equation).

4.1.4 Does physiology have that outcome?

To test that, we incorporated the Golgi cell ensemble conversion into a model that recodes mossy fibre signals into granule cell signals. The model compares mossy fibre

signal frequency with inhibition at each of 4 dendrites of each of 8,750 granule cells per field, in each of 100 fields. Mossy fibre input rates to each field are derived per section 3 and Methods, so taking into account, *inter alia*, that a field receives a randomly variable number of copies of most signals, and most terminal clusters lie only partly inside a field. Inhibition – outputs of the ensemble conversion, 700 per field – is provided by the Golgi cell model. Excitation and inhibition received by each glomerulus are randomly paired. Pairing is used to identify the subset of granule cells that fire (cells that receive at least 3 mossy fibre signals which exceed the inhibitory threshold). Output of the model is the number of granule cells that fire in each field, the mean of mossy fibre rates they each receive (the sample means), and the mean of the sample means in each field ('field means'). The results are shown in Figure 4.

4.1.5 Results

Feed-forward inhibition – mossy fibre → Golgi cell → granule cell – reliably and closely regulates the fraction of granule cells that are active at low density. The Golgi cell computation may be the primary regulator of the number of granule cells that fire. Field-to-field random variability of the number is inversely proportional to the fraction that are active, suggesting that, if primary regulation is in this form, the fraction is low. We would nonetheless expect to see greater precision, suggesting the physiological presence of a supplementary mechanism(s) that we have not represented in the model.

389 A local feedback mechanism may be provided by granule cell ascending axon contact
390 on Golgi cells. The ascending portion of the granule cell axon makes synaptic contact
391 on local Golgi cells, on basal dendrites [11]. A Golgi cell receives ~400 functional
392 synaptic contacts from this source, around 25% of the granule cells that a Golgi cell
393 receives contact from in total. During sustained mossy fibre discharge, synapses from
394 local granule cells contribute equivalent charge to Golgi cells as mossy fibre synapses
395 and 'display similarly fast kinetics' [42]. Short-latency inhibitory feedback may add
396 homeostatic fine adjustment to regulation at local level, at field scale.

397 It is a long-standing idea [43] that granule cell activity may be regulated by feedback
398 via parallel fibres, which contact Golgi cell apical dendrites. We have previously
399 proposed that gap junctions between apical dendrites may provide the means for
400 Golgi cells to detect the density of parallel fibre activity [44]. Feedback by this pathway
401 is not sensitive to local fluctuation of granule cell active numbers, and may be the
402 weakest regulator.

403 The results are the same with any (tested) distribution of mossy fibre rates and also
404 whether mossy fibres are all active or some are active and others are not. Active cells
405 can be in any random permutation.

406 **Figure 4**

407

4.2 Granule cells encode mossy fibre rate information collectively in rank-sized strips

4.2.1 Hypothesis

Anatomy simulates independent random sampling by a single granule cell of the population of mossy fibre input rates to the whole rank (section 2). The granule cell firing rate is a linear function of depolarising somatic charge, in turn a linear function of the mean (or sum) of dominant excitatory input rates. The linear relationship is undiluted by inhibition because dominant signals transiently displace a significant effect of inhibition. Derived in this way, granule cell rates are collectively well predicted by mossy fibre rates, by the central limit theorem. This provides the substrate for granule cells to collectively encode mossy fibre rate information. Code groups are functionally defined by the topography of mossy fibre input to the cerebellum, as Golgi cell networks are. The output of a rank is the smallest unit of granule cell encoded information. The permutation of active mossy fibres, and of granule cells, and how firing rates are distributed among active cells, all code nothing.

4.2.2 Do granule cell firing rates – the output of a rank – have the hypothesised features?

We ran the same simulation as section 4.1 to test whether, and how, mossy fibre rates are related to granule cell rates, and if fields in a rank all have the same output. We take granule cell firing rates to be a linear function of the mean of dominant input rates to each active cell, which we take as the mean itself. Field means are therefore the mean of granule cell firing rates in each field. The results are shown in Figures 5 and 6. We present evidence relating to mossy fibre → granule cell linear transmission in the Methods section (Methods, Linear transmission of mossy fibres to granule cells).

The narrowing and predicted shape of the granule cell frequency distribution is evident in all conditions. The field means approach a straight line, the test that a rank operates as a single functional unit. When mossy fibre rates are normally distributed (SD 12.5 Hz), the granule cell distribution is very narrow (and normal if rates are counted in narrower bins) and the field means are very close to a straight line. The field means follow the mean of mossy fibre rates at a precisely fixed distance. When mossy fibre rates have a random uniform distribution, the field means remain almost a straight line, and the distance from the mossy fibre mean varies with the size of the mossy fibre range.

A straight line indicates that fields all return the same output – not the same firing rates, but the same narrowed range, clustered around the mean, and attracted to a normal distribution (more evident with narrowly and/or normally distributed mossy fibre rates). This holds even though a single granule cell receives a tiny fraction of mossy fibre rates, and each field receives only a small random sample of mossy fibre signals received by a rank, and regardless of the shape of the mossy fibre distribution.

This is not in itself necessarily in fatal conflict with the traditional cerebellar learning model, but has the alternative interpretation that granule cell firing conserves mossy fibre rate information, coded in the output of a whole rank. This is therefore the minimum resolution of granule cell information, but not the minimum unit of code. The same information is coded in any random sample of granule cell signals over a modest minimum number. It is immaterial (i.e. codes nothing) which particular cells are active or which cells fire at what rates, or even what rates those are, provided any random sample of rates is as if drawn from the same frequency distribution, with replacement. The output of a rank can be likened by analogy to a pixel: it is only divisible into smaller pieces of the same information.

Figures 5 and 6

5. Discussion

There is a general expectation that the representation of information in the brain is in high resolution and replicable with high fidelity, and that those features make it precise and provide the inputs to sophisticated computations. We challenge that. We propose in this paper:

i) There is a computational effect, unaided and unlearned, of the triad of cell morphologies, network architecture and linear transmission, for which the granular layer is highly adapted.

ii) Recoding in the granular layer exploits the central limit theorem. Statistical properties of granule cell rates code mossy fibre rate information. The pattern of active granule cells, and which cells fire at what rates, code nothing.

iii) High-dimensional mossy fibre information recodes as a very low-resolution granule cell code. Large cell groups code information in their collective activity. At any instant, a whole group codes the same information. A code group functions as a single unit and spans the cerebellar network sagittally. So, information has spatial dimensions, the dimensions of a code group.

477 iv) Granule cell code groups mirror microzonal organisation of the molecular layer.
478 Accordingly, granule cell encoded information has a striped pattern viewed from the
479 cerebellar surface. This can be likened by analogy to pixellation.

480 v) While firing of a whole code group is the minimum unit of information, it is not the
481 minimum unit of code. Inside pixel boundaries the same information is coded in any
482 random sample of granule cell firing rates.

483 vi) There is a huge sacrifice of data resolution on entry to the cerebellum, counter to
484 the general expectation that more data should inform more powerful brain
485 computations. This is functional. Coded in this form, granule cell data can drive
486 coherent firing of large cell groups downstream. Microzones lie at right angles to
487 parallel fibres, presenting a large target. The form of the granule cell code means the
488 same information is received by all locations of sagittal plane, so that microzone-
489 grouped Purkinje cells receive the same information without receiving the same
490 signals. An estimated 350,000 parallel fibres pass through a Purkinje cell dendritic
491 territory [45-48]. If even only a small fraction of parallel fibres is active (0.5%), and
492 allowing for the fact that only one in two make contact, and that a majority of
493 synapses are severely depressed or silent [49, 50], a single Purkinje cell still receives
494 around 200 parallel fibre signals at working synapses at any time. A granule cell code in
495 this form provides a means to modulate firing of Purkinje cells in unison by a chain of

496 rate codes. There is evidence that Purkinje cells linearly code the strength of granule
497 cell inputs [6-8] and behavioural metrics [3, 51-54].

498 vii) A statistical code may be a physiological strategy to mitigate variable performance
499 of single neurons and synapses, a long-known impediment to precise and replicable
500 biological information capture. Learning models depend on pattern replication for
501 signals to match up with the correct synaptic weights. Yet it is known that single cells
502 are not metronomically consistent performers. The response of cells of the same type
503 can vary in the same conditions, and so can the response of a single cell to the same
504 stimulus at different times. Moreover, the granular layer is *designed* to amplify the
505 difference if the pattern of active mossy fibres should vary only by a modest number of
506 cells. Indeed, even that is not necessary – the same cells firing at different rates also
507 generates a different pattern of active granule cells, and therefore parallel fibres. Small
508 differences of input are converted by decorrelation to wholesale changes to output.
509 Possibly, and we submit, the cerebellum actively eschews reliance on pattern
510 replication in favour of group code which gives a more (because statistically) reliable
511 outcome.

512 A perennial issue for network theory is that biological networks do not seem to have
513 much information about the signals they receive. Input to the cerebellum is eclectic
514 and in multiple modalities. In some cases, a single granule cell can receive multi-modal
515 input. In the traditional cerebellar model, supervision solves this problem. It is

516 unnecessary for the cerebellum itself to discriminate because it is an assumption of the
517 model that externally sourced instruction signals train the correct response.

518 We propose instead the solution that resolution of high-dimensional input data is
519 sacrificed. The cerebellum disregards source and modality data below a physical scale
520 which mirrors topography. It is therefore unnecessary to discriminate below that scale.
521 Mapping studies show that mossy fibre signals (evoked by cutaneous stimulation)
522 share the topographical organisation of climbing fibres [55-57]. At sub-topographical
523 dimensions, signal source and type are simply discounted. Therefore, networks do not
524 need to be adapted to the source or type of input they receive – anatomically,
525 networks are interchangeable, so network design can be modular. This feature makes
526 it functionally flexible, allowing the almost unchanging basic cerebellar wiring to
527 survive dramatic upheavals of the vertebrate phenotype [58, 59].

528

529 **METHODS**

530 **DERIVATION OF MOSSY FIBRE RATES**

531 **The number of mossy fibres that innervate a rank**

532 As far as is known, fields receive a random sample mossy fibre input rates to a rank. To
533 simulate that, we need the size of the sampled population – the number of mossy fibre signals
534 received by a rank – and sample size, the number received by a field.

535 Despite the repeating 'crystalline' architecture of the cerebellar cortex, at local level there are
536 anatomical random variables. Variables are: i) the number of mossy fibres that innervate a
537 field, ii) the number of terminals they each end in, and iii) the number of those that are inside
538 field limits.

539 The number of mossy fibres afferent to a field has been estimated at 100 [20]. However, that
540 number is a field-sized fraction of the general population. The actual number is larger because
541 mossy fibres end in a dispersed group (cluster) of terminals, and most groups straddle field
542 limits.

543 We work from an estimate of the total number of terminals per field, which is, in turn, derived
544 from convergent estimates of the number of granule cells per field. (Estimate 1) There are an
545 estimated 1.92×10^6 granule cells per µl [45]. The number of fields which fit in that volume is
546 $(1{,}000/150)^2 \times (1{,}000/200) = \sim 222$, assuming a field depth of 150 µm [20]. The number of
547 granule cells in a field is, therefore 1,920,000/222 = 8,649. (Estimate 2) An estimated 350,000
548 parallel fibres pass through a single Purkinje cell's territory [45]. Parallel fibres run about 3 mm
549 in each direction from the granule cell soma [60, 61]. The Purkinje cell dendritic arbour fills the
550 molecular layer vertically and averages ~200 µm wide. Therefore, 6,000/150 = 40 fields fit in a
551 row that provides parallel fibres that pass through a Purkinje cell dendritic territory, giving
552 350,000/40 = 8,750 granule cells per field. Estimates vary of the number of granule cells which
553 extend a dendrite into a single glomerulus. 50 is mid-range. (8,750/50) x 4 = 700 glomeruli per
554 field.

555 Granule cells have 3–5 dendrites, averaging 4, and receive input to each of them from a single
556 mossy fibre (so an average granule cell receives 4 inputs). Estimates of divergence of a single
557 mossy fibre terminal onto granule cells vary [2]. It is unclear how much this reflects biological
558 diversity versus differences in opinion and methods. Here we use a mid-range estimate of 1:50
559 [34, 35]. Assuming a mossy fibre terminal receives a single granule cell dendrite from each of d
560 granule cells, and given an average of 4 dendrites per granule cell and z granule cells per field,
561 the total number of mossy fibre terminals in a field is $N = (z \times 4)/d = 700$ given $z = 8{,}750$ and d
562 $= 50$. A convergent estimate is provided by multiplying the per field number of mossy fibres by
563 the average number of terminals per cluster.

564 Cluster size varies. We take the range as 4–12 terminals per cluster [20]. We assume the
565 number varies at random and cluster sizes occur with equal probability. A maximum of 7 fits in
566 a field (because a field shares the dimensions of the area that encloses a mean cluster). Fields
567 are not anatomically bounded, so many clusters straddle field limits. To reflect that, we
568 assume there is a 1/7 probability that a 7-terminal cluster (or larger) has 7 terminals inside a
569 field and also the same probability of any other number. A 6-terminal cluster has a 2/7 chance
570 that all 6 terminals are inside and a 1/7 chance of any other number, and so on.

571 Table 1 shows the derivation of the expected (i.e., predicted by probability) ratios of terminals
572 contributed to a field by each cluster size (R1), not counting terminals that lie outside when a
573 cluster straddles field boundaries; and the ratios of mossy fibres contributing $n = 1$–7 terminals
574 (R2), regardless of cluster size. R1 ratios are given by the sum of numbers in each row. So, for
575 example, the ratio of cells that end in 8 terminals to cells that end in 5 is 28:25. R2 ratios are
576 given by the number of appearances of each number in the grid – so the expected ratio of cells
577 which contribute 7 terminals to the number which contribute 4 is 6:12. The ratios effectively
578 give the distributed probability of possible states. For example, there is a probability of 10/(6 +
579 8 + 10 + 12 + (3 x 9)) = 0.159 that a mossy fibre contributes 5 terminals to a field (regardless of
580 cluster size). Similarly, there is a probability of ((6 x 28)/((6 x 28) + 27 + 25 + 22))/7 = 0.099 that
581 a given cell contributes 7 terminals to a field.

582

583

584 **Table 1. Derivation of expected ratios**

size	number of terminals inside							R1
12	7	6	5	4	3	2	1	**28**
11	7	6	5	4	3	2	1	**28**
10	7	6	5	4	3	2	1	**28**
9	7	6	5	4	3	2	1	**28**
8	7	6	5	4	3	2	1	**28**
7	7	6	5	4	3	2	1	**28**
6	6	6	5	4	3	2	1	**27**
5	5	5	5	4	3	2	1	**25**
4	4	4	4	4	3	2	1	**22**
R2	6	8	10	12	9	9	9	

585

586 If R1 ratios are denoted by a series $x_4, x_5 \ldots x_{12}$, and a given element in the series is x_j, the
587 fraction of terminals provided by a given cluster size is $x_j/(x_4 + x_5 + \cdots + x_{12})$, and this
588 fraction is multiplied by N to give the number of terminals. The number of terminals is divided
589 by the expected mean number of terminals that fall inside field limits (for that cluster size) to
590 give the expected number of mossy fibres that provide them. The number of j-terminal mossy
591 fibres that innervate a field is therefore given by

$$N\left[{x_j}\Big/{\textstyle\sum_{i=1}^{n} x_i}\right]\Big/\left[{x_j}/{7}\right]$$

592 The results are shown in Table 2. The equal number of mossy fibres (mfs) in each column is
593 what we would expect, because we made it an assumption that all sizes occur with equal
594 probability, and mf values are expected values – i.e., in proportions predicted by their

probability. The mf total is the expected number of mossy fibres afferent to a field (which contribute at least one terminal).

Table 2. The expected number of mossy fibres which innervate a field

cluster size	12	11	10	9	8	7	6	5	4	total
terminals	81	81	81	81	81	81	78.1	72.3	63.6	700
mfs	20.25	20.25	20.25	20.25	20.25	20.25	20.25	20.25	20.25	182.25

R2 ratios – the relative incidence of afferent mossy fibres that contribute 7 terminals to a field, 6 terminals, 5 and so on, down to 1 – and the expected number of mossy fibres that contribute them, are shown in Table 3.

Table 3. The number of mossy fibres which contribute *n* = 1–7 terminals to a field

n	7	6	5	4	3	2	1	total
R2	6	8	10	12	9	9	9	63
R3	42	48	50	48	27	18	9	
mfs	17.34	23.15	28.92	34.72	26.04	26.04	26.04	182.25
%age	9.52	12.69	15.87	19.05	14.29	14.29	14.29	

R3 is *n* x R2, giving the ratio of terminals provided by mossy fibres with *n* terminals inside a field. %age is given by (R2/63) x 100. this is the percentage of mossy fibres with *n* terminals inside a field.

From here, the number of mossy fibres that innervate a rank is given by 182.25 x 100 divided by the mean number of clusters per mossy fibre per rank. If a rank receives, on average, five clusters per mossy fibre, ~3,645 mossy fibres innervate a rank. This is the estimate used in the simulation unless stated otherwise.

Assumptions. Cluster sizes occur with equal probability. The probabilities of each outcome when a cluster straddles field boundaries (how many terminals are inside and how many outside) are as stated. A single mossy fibre ends in an average of 5 terminal clusters per rank.

Mossy fibre input rates to a field

Terminal clustering means a field receives multiple copies of most signals. The proportions of mossy fibres afferent to a simulated field that contribute each possible number of terminals (1–7) are generated in simulated steps. In the first step, the simulation randomly generates, for each field, the cluster size ratio. This means, the relative proportions of afferent mossy fibres (which contribute at least 1 terminal to a field) that end in 4 terminals, 5, 6 and so on up to 12, assuming they occur with equal probability, disregarding how many terminals fall inside and outside field boundaries. In step two, the ratio of cluster sizes is weighted to reflect the greater probability that large clusters contribute more terminals to a field. In step 3, ratios are converted to the fraction of terminals contributed by each cluster size. When multiplied by the total number of terminals, this gives the number of terminals contributed by each cluster size. In step four, the values obtained in step three are divided up between cells that contribute a single terminal, 2 terminals, 3 and so on, to reflect straddling of field limits. The proportions give the number of mossy fibres afferent to a simulated field that contribute a single terminal, two, three and so on up to seven, the maximum.

There is no field-level effect of mossy fibre terminal branching. Terminal clusters arising from the same mossy fibre are separated by a minimum distance, so that a field cannot contain terminals of more than one cluster per mossy fibre.

Terminal clustering means that fields contain a randomly variable number of copies of most signals. In the simulation, copies are added after sampling of mossy fibre rates to obtain rates received by a field. An alternative order would be to add copies to the sampled population and then sample that. We follow anatomy: the number of *rates* received by a field is equal to the number of afferent mossy fibres; the number of *signals* contains duplicate rates.

DERIVATION OF ENSEMBLE DIMENSIONS AND MODEL PARAMETERS

4 Purkinje cells fit in a field, based on field size, thickness of the Purkinje cell dendritic plate – 9 µm [62] – and the distance between them – ~40 µm [63]. ‘In man, the ratio [of Purkinje cells to Golgi cells] is 1:1.5, while in the monkey and cat it is almost 1:1.9 and in the rat 1:3.3’ [64].

640 Possibly, estimates are low because smaller Golgi cells at deeper level were not counted [63
641 p.121]. We take it that there are 10 Golgi cells per field, a ratio of 1:2.5 with 4 Purkinje cells.

642 Golgi cell morphology creates ensemble dimensions. The Golgi cell axon ramifies profusely,
643 giving rise to a dense plexus. The axonal field is sagittally elongated – that is, in the direction of
644 the long axis of a microzone (mean range 650 +/- 179 µm by 180 +/- 40 µm [in mice: 65]) – and
645 is the depth of the granular layer, which it fills vertically. Fine, beaded axon fibres enter
646 glomeruli, where they inhibit granule cells [66]. Because of the dimensions and orientation of
647 the Golgi cell plexus, all Golgi cells in a sagittal row of three fields inhibit substantially the
648 whole of the middle field. Each field defines a functional population of Golgi cells – an
649 ensemble – being those cells with convergent input to that field. A single Golgi cell contacts
650 thousands of granule cells [66, 67].

651 Contact by mossy fibres on a Golgi cell is on basal dendrites. 4–6 basal dendrites arise from the
652 Golgi cell soma. We assume 5, so a population of ensemble-grouped Golgi cells has a
653 combined total of 30 x 5 = 150 basal dendrites. The number of mossy fibres which contact a
654 Golgi cell is unreported. Dendrites radiate from the cell body. A single dendrite has a range of
655 50–100 µm [63]. The longest dimension of a field – which contains ~700 mossy fibre terminals
656 – is 200 µm. We estimate the mean number of mossy fibres that contact a single dendrite is 4,
657 so 20 per cell, or ~3% of the population of terminals (or 0.6% per dendrite).

658 Glomeruli individually receive innervation from a random sample of Golgi cells afferent to a
659 field. It is unknown how many Golgi cells innervate a glomerulus.

660

661 **LINEAR TRANSMISSION OF MOSSY FIBRES TO GOLGI CELLS**

662 It is part of our proposal that Golgi cell basal dendritic signals linearly reflect mossy fibre rates,
663 so that mossy fibre rate information is conserved proportionally in Golgi cell firing rates. Golgi
664 cells are large interneurons whose cell bodies and basal dendrites lie in the granular layer.
665 Mossy fibres directly contact Golgi cell basal dendrites. Golgi cell firing frequency increases
666 linearly with the amplitude of depolarising current [29 p.845]. 'Golgi cells can follow peripheral

667 signals in a continuous fashion, modulating their frequency with the intensity of the stimulus
668 [citing [68, 69]]' [70]. As a result, during movement, the 'output of Golgi cells varies smoothly
669 as a function of input.…They are capable of modulating their output to reflect their input with
670 little noise or signal distortion' [12]. 'Sensory-evoked Golgi-cell inhibition scales proportionally
671 with the level of mossy fiber excitatory synaptic input', such that inhibition reliably conveys
672 mossy fibre rate information [4]. On this evidence: mossy fibre rate information is conserved
673 proportionally in Golgi cell firing rates.

674 Golgi cells extend their basal dendrites into glomeruli [66, 71]. Contact on them by mossy
675 fibres is multi-synaptic [63], contributing to a reliable, rapid (submillisecond) response. The
676 fast rise time and weak distance dependence of the amplitude and timing of Golgi cell EPSCs
677 evoked by mossy fibre signals, suggests that basal dendrites introduce relatively little filtering
678 [11, 28], as expected for large-diameter dendrites. We note that the pause in Golgi cell firing
679 following a discrete stimulus under anaesthesia [4, 72, 73] disappears from Golgi cell
680 recordings during locomotion [69].

681 During behaviour in freely-moving animals, mossy fibre activity is dense: a high fraction of
682 mossy fibres are active [74]. Both mossy fibres [75-77] and Golgi cells [69] have been reported
683 to fire with a sustained, time-varying signature. In the behaving animal, Golgi cell basal
684 dendritic membrane potential is a continuous variable under modulation by sustained inputs,
685 we submit. As charge transfer to the soma is passive, polarisation of the soma is likewise
686 sustained, under modulation by dendritic states.

687 It is worth noting that very high mossy fibre rates can be generated in experimental conditions.
688 However, the typical physiological range is 50–300 Hz [76]. In the simulations, we use the
689 physiological rates, within stated constraints on the shape of the distribution.

690 **Other control of Golgi cells?** Do Golgi cells receive a significant influence of input from other
691 sources? The evidence is incomplete but currently suggests other influence is absent or weak.
692 Contrary to early reports, neither Purkinje cells nor climbing fibres contact Golgi cells [78, who
693 give references], and only a modest minority of inhibitory inputs to Golgi cells (if any) are from
694 molecular layer interneurons [79], which generate weak synaptic currents [80], consistent with

695 either extremely weak or wholly absent innervation [81]. There is conflicting evidence whether
696 Golgi cells make inhibitory synaptic contact on each other [81, 82]. Our simulation does not
697 include an effect on Golgi cell firing by other sources of input.

698

699 **LINEAR TRANSMISSION OF GOLGI CELLS TO GRANULE CELLS**

700 'In the adult rat cerebellum, each granule cell dendrite receives 2.6 ± 0.55 synaptic contacts
701 from Golgi axon terminals' [30] citing [35].[1] However, the large majority of inhibition (98%) is
702 by spillover [5], where neurotransmitter released into the synaptic cleft spills out into the
703 glomerular space. Golgi cells release GABA, an inhibitory neurotransmitter. This is detected by
704 high-affinity $GABA_A$ receptors located perisynaptically and extrasynaptically on granule cells
705 [31, 32]. Even synaptically-received signals have most of their effect (i.e., the large majority of
706 charge transfer is mediated) via spillover.[2]

707 Golgi cells fire spontaneously [83] at a time-varying rate in the behaving animal, so that
708 downstream, a glomerulus receives continuous convergent input. As a result, there is a
709 sustained build-up of glomerular GABA during behaviour [84] at an adjustable concentration
710 controlled by the mean of afferent Golgi cell firing rates [85]. A glomerulus randomly samples
711 Golgi cells afferent to a field. Golgi cells provide the only inhibitory input to granule cells.

712 Signalling by spillover is sometimes assumed to be ambient and slow. However, the action of
713 glomerular GABA spillover has a fast phasic component – not as fast as synaptic transmission
714 (~1 ms) but with a rise time of only a few milliseconds [85]. Unlike the spiky appearance of
715 synaptically-induced inhibitory postsynaptic currents, spillover [4] generates a sustained

---

[1] Data are sparse. The original data are an estimate derived from visual inspection of slices thirty years ago so far without later corroboration, except from Rossi and Hamann 1998, who derive a lower estimate but propose the disparity is because their estimate is too low.

[2] Because of the long duration of IPSCs generated by spillover (recorded in slices), the total charge carried is three times that of IPSCs generated by directly connected terminals. 30. Rossi, D.J. and M. Hamann, *Spillover-mediated transmission at inhibitory synapses promoted by high affinity alpha6 subunit GABA(A) receptors and glomerular geometry.* Neuron, 1998. **20**(4): p. 783-95.

716 outward current. The response time to multiple inputs is likely faster than the experimentally
717 isolated response to a discrete signal (because the combined rate of GABA release is higher).

718 **Golgi cell oscillations.** Golgi cells fire autonomously. Under anaesthesia, firing falls into a slow
719 oscillating pattern [86]. Under excitatory synaptic input, however, this disappears [82].
720 Anaesthesia 'has a strong influence on spontaneous activity of Golgi cells' [78]. Discharge at
721 low rates with irregular timing under anaesthesia [83] is replaced by higher rates with more
722 regular timing without anaesthesia [68, 69, 87]. (This paragraph is a cautionary note about
723 evidence obtained under anaesthesia, which has been used to argue that oscillations provide a
724 form of signalling.)

725

726 **LINEAR TRANSMISSION OF MOSSY FIBRES TO GRANULE CELLS**

727 There is significant evidence that granule cell firing rates are linearly related to input rates, but
728 also evidence thought to be unfavourable to that conclusion. We take them in turn.

729 The short and equal length of granule cell dendrites would suggest light and equal filtering.
730 The mossy fibre-granule cell connection has a range of adaptations which support high-fidelity
731 transmission of high frequency signals across a wide bandwidth [9]. Faithful transmission of
732 rate information is reported [1, 2]. Vesicle release and replenishment are fast [10, 13] and
733 postsynaptic AMPA receptors operate in their linear range [13], where they are resistant to
734 desensitisation [88]. Multiple contacts are made by a mossy fibre with each granule cell [35].
735 Conversion of depolarising somatic charge into granule cell firing is a simple function, such that
736 granule cells 'have a relatively linear and uncomplicated conversion of depolarisation level to
737 spike rate' [41 p.2393, citing Jorntell and Ekerot 2006 and D'Angelo et al 1998].

738 Glutamate spillover enhances precision and reliability of transmission [13, 89]. During
739 behaviour, at sustained physiological mossy fibre rates, there may be a build-up of
740 intraglomerular glutamate, increasing the relative influence of spillover in a balance with
741 synaptic transmission, assisted by short-term synaptic depression. In these conditions,
742 spillover may dominate, as it dominates inhibitory transmission [5, 85]. Spillover from multiple

743 release sites (200-400 at a single mossy fibre terminal) is plausibly sufficient to mitigate
744 variability of vesicular size, release probability, and the number of release points at synapses
745 made on any individual cell, increasing fidelity and equality of excitation of granule cells.

746 Against that, there are reported to be heterogeneous synaptic weights. Different strength and
747 short-term dynamics of the mossy fibre to granule cell connection have been reported in
748 vestibular slices, with $GABA_A$ receptors blocked. The amplitude of the response, measured at
749 the soma, is reported to be statistically correlated to the source of the mossy fibre that is
750 stimulated [90], suggesting that the strength of the connection depends on the source.

751 However, the presence of weights does not necessarily mean that the function is to modulate
752 firing rates. Rather, it is suggested that the function may temporally code the source of inputs
753 because different combinations have different response onset times. An alternative, which
754 they also mention, is that some inputs may be in a supporting role, reminiscent of 'driver' and
755 'modulatory' signals in the thalamus and cortex [91]. Feasibly, signals in a supporting role must
756 be present for the postsynaptic granule cell to fire, but do not affect the granule cell firing rate.

Grants

Funding: This work was supported by the Leverhulme Trust [grant number ECF-2022-079] (Mike Gilbert); the Swedish Research Council [grant number 2020-01468]; the Per-Eric och Ulla Schybergs Foundation [grant number 42630]; and the Crafoord Foundation [grant numbers 20180704, 20200729, 20220776, & 20230655] (Anders Rasmussen).

Acknowledgement

Dr Mike Evans, School of Mathematics, University of Leeds, LS2 9JT, UK, read an early draft of the paper and provided feedback.

Author contributions

M.G. Researched, conceived and developed the ideas, performed the analysis, wrote the code, prepared the figures and wrote the manuscript. A.R. provided expertise and feedback, and reviewed and provided editorial comments on the manuscript.

Declaration of interests

The authors declare no competing interests.

REFERENCES

1. Rancz, E.A., et al., *High-fidelity transmission of sensory information by single cerebellar mossy fibre boutons.* Nature, 2007. **450**(7173): p. 1245-8.
2. Ritzau-Jost, A., et al., *Ultrafast action potentials mediate kilohertz signaling at a central synapse.* Neuron, 2014. **84**(1): p. 152-163.
3. Jelitai, M., et al., *Dendritic excitation-inhibition balance shapes cerebellar output during motor behaviour.* Nat Commun, 2016. **7**: p. 13722.
4. Duguid, I., et al., *Control of cerebellar granule cell output by sensory-evoked Golgi cell inhibition.* Proc Natl Acad Sci U S A, 2015. **112**(42): p. 13099-104.
5. Duguid, I., et al., *Tonic inhibition enhances fidelity of sensory information transmission in the cerebellar cortex.* J Neurosci, 2012. **32**(32): p. 11132-43.
6. Walter, J.T. and K. Khodakhah, *The linear computational algorithm of cerebellar Purkinje cells.* J Neurosci, 2006. **26**(50): p. 12861-72.
7. Walter, J.T. and K. Khodakhah, *The advantages of linear information processing for cerebellar computation.* Proc Natl Acad Sci U S A, 2009. **106**(11): p. 4471-6.
8. Park, S.M., E. Tara, and K. Khodakhah, *Efficient generation of reciprocal signals by inhibition.* J Neurophysiol, 2012. **107**(9): p. 2453-62.
9. Delvendahl, I. and S. Hallermann, *The Cerebellar Mossy Fiber Synapse as a Model for High-Frequency Transmission in the Mammalian CNS.* Trends Neurosci, 2016. **39**(11): p. 722-737.
10. Saviane, C. and R.A. Silver, *Fast vesicle reloading and a large pool sustain high bandwidth transmission at a central synapse.* Nature, 2006. **439**(7079): p. 983-7.
11. Cesana, E., et al. *Novel granule cell-Golgi cell excitatory input in the cerebellar granular layer*. in *FENS Abstr*. 2010.
12. Moore, J.W. and D.E.J. Blazis, *11 - Simulation of a Classically Conditioned Response: A Cerebellar Neural Network Implementation of the Sutton–Barto–Desmond Model*, in *Neural Models of Plasticity*, J.H. Byrne and W.O. Berry, Editors. 1989, Academic Press. p. 187-207.
13. Sargent, P.B., et al., *Rapid vesicular release, quantal variability, and spillover contribute to the precision and reliability of transmission at a glomerular synapse.* J Neurosci, 2005. **25**(36): p. 8173-87.
14. Turecek, J., S.L. Jackman, and W.G. Regehr, *Synaptic Specializations Support Frequency-Independent Purkinje Cell Output from the Cerebellar Cortex.* Cell Reports, 2016. **17**(12): p. 12.
15. Turecek, J., S.L. Jackman, and W.G. Regehr, *Synaptotagmin 7 confers frequency invariance onto specialized depressing synapses.* Nature, 2017. **551**: p. 503.
16. Raymond, J.L. and J.F. Medina, *Computational Principles of Supervised Learning in the Cerebellum.* Annu Rev Neurosci, 2018. **41**: p. 233-253.
17. Alvina, K., et al., *Questioning the role of rebound firing in the cerebellum.* Nat Neurosci, 2008. **11**(11): p. 1256-8.
18. Schonewille, M., et al., *Purkinje cells in awake behaving animals operate at the upstate membrane potential.* Nat Neurosci, 2006. **9**(4): p. 459-61; author reply 461.

19. Wu, H.S., I. Sugihara, and Y. Shinoda, *Projection patterns of single mossy fibers originating from the lateral reticular nucleus in the rat cerebellar cortex and nuclei.* J Comp Neurol, 1999. **411**(1): p. 97-118.
20. Sultan, F. and D. Heck, *Detection of sequences in the cerebellar cortex: numerical estimate of the possible number of tidal-wave inducing sequences represented.* J Physiol Paris, 2003. **97**(4-6): p. 591-600.
21. Shinoda, Y. and I. Sugihara, *Axonal Trajectories of Single Climbing and Mossy Fiber Neurons in the Cerebellar Cortex and Nucleus*, in *Handbook of the Cerebellum and Cerebellar Disorders*, S.J.D. Manto M., Rossi F., Gruol D.L., Koibuchi N., Editor. 2013, Springer, Dordrecht.
22. Shinoda, Y., et al., *The entire trajectory of single climbing and mossy fibers in the cerebellar nuclei and cortex.* Prog Brain Res, 2000. **124**: p. 173-86.
23. Garwicz, M., C.F. Ekerot, and H. Jorntell, *Organizational principles of cerebellar neuronal circuitry.* News in Physiological Sciences, 1998. **13**: p. 28-34.
24. Oscarsson, O., *Functional units of the cerebellum - sagittal zones and microzones.* Trends in Neurosciences, 1979. **2**: p. 143-145.
25. Ozden, I., et al., *Reliable coding emerges from coactivation of climbing fibers in microbands of cerebellar Purkinje neurons.* J Neurosci, 2009. **29**(34): p. 10463-73.
26. Dean, P., et al., *The cerebellar microcircuit as an adaptive filter: experimental and computational evidence.* Nat Rev Neurosci, 2010. **11**(1): p. 30-43.
27. Eccles, J.C., M. Ito, and J. Szentágothai, *The cerebellum as a neuronal machine*. 1967, Berlin, New York etc.: Springer-Verlag. 335 p.
28. Kanichay, R.T. and R.A. Silver, *Synaptic and cellular properties of the feedforward inhibitory circuit within the input layer of the cerebellar cortex.* J Neurosci, 2008. **28**(36): p. 8955-67.
29. Dieudonné, S., *Submillisecond kinetics and low efficacy of parallel fibre-Golgi cell synaptic currents in the rat cerebellum.* J Physiol, 1998. **510 (Pt 3)**: p. 845-66.
30. Rossi, D.J. and M. Hamann, *Spillover-mediated transmission at inhibitory synapses promoted by high affinity alpha6 subunit GABA(A) receptors and glomerular geometry.* Neuron, 1998. **20**(4): p. 783-95.
31. Nusser, Z., W. Sieghart, and P. Somogyi, *Segregation of different GABAA receptors to synaptic and extrasynaptic membranes of cerebellar granule cells.* J Neurosci, 1998. **18**(5): p. 1693-703.
32. Brickley, S.G., S.G. Cull-Candy, and M. Farrant, *Development of a tonic form of synaptic inhibition in rat cerebellar granule cells resulting from persistent activation of GABAA receptors.* J Physiol, 1996. **497 (Pt 3)**: p. 753-9.
33. Gilbert, M. and R.C. Miall, *How and Why the Cerebellum Recodes Input Signals: An Alternative to Machine Learning.* Neuroscientist, 2021a. **DOI: 10.1177/1073858420986795**.
34. Gao, Z., et al., *Excitatory Cerebellar Nucleocortical Circuit Provides Internal Amplification during Associative Conditioning.* Neuron, 2016. **89**(3): p. 645-57.
35. Jakab, R.L. and J. Hámori, *Quantitative morphology and synaptology of cerebellar glomeruli in the rat.* Anat Embryol (Berl), 1988. **179**(1): p. 81-8.

857 36. Mitchell, S.J. and R.A. Silver, *GABA spillover from single inhibitory axons suppresses*
858 *low-frequency excitatory transmission at the cerebellar glomerulus.* J Neurosci, 2000a.
859 **20**(23): p. 8651-8.
860 37. Mitchell, S.J. and R.A. Silver, *Glutamate spillover suppresses inhibition by activating*
861 *presynaptic mGluRs.* Nature, 2000b. **404**(6777): p. 498-502.
862 38. Billings, G., et al., *Network structure within the cerebellar input layer enables lossless*
863 *sparse encoding.* Neuron, 2014. **83**(4): p. 960-74.
864 39. Jörntell, H. and C.F. Ekerot, *Properties of somatosensory synaptic integration in*
865 *cerebellar granule cells in vivo.* J Neurosci, 2006. **26**(45): p. 11786-97.
866 40. Chadderton, P., T.W. Margrie, and M. Hausser, *Integration of quanta in cerebellar*
867 *granule cells during sensory processing.* Nature, 2004. **428**(6985): p. 856-60.
868 41. Bengtsson, F. and H. Jörntell, *Sensory transmission in cerebellar granule cells relies on*
869 *similarly coded mossy fiber inputs.* Proc Natl Acad Sci U S A, 2009. **106**(7): p. 2389-94.
870 42. Cesana, E., et al., *Granule cell ascending axon excitatory synapses onto Golgi cells*
871 *implement a potent feedback circuit in the cerebellar granular layer.* J Neurosci, 2013.
872 **33**(30): p. 12430-46.
873 43. Albus, J.S., *A Theory of Cerebellar Function.* Mathematical Biosciences, 1971. **10**(1-2):
874 p. 25-61.
875 44. Gilbert, M. and A. Rasmussen, *Gap Junctions May Have A Computational Function In*
876 *The Cerebellum: A Hypothesis.* The Cerebellum, 2024.
877 45. Harvey, R.J. and R.M. Napper, *Quantitative study of granule and Purkinje cells in the*
878 *cerebellar cortex of the rat.* J Comp Neurol, 1988. **274**(2): p. 151-7.
879 46. Harvey, R.J. and R.M. Napper, *Quantitative studies on the mammalian cerebellum.*
880 Prog Neurobiol, 1991. **36**(6): p. 437-63.
881 47. Napper, R.M. and R.J. Harvey, *Number of parallel fiber synapses on an individual*
882 *Purkinje cell in the cerebellum of the rat.* J Comp Neurol, 1988. **274**(2): p. 168-77.
883 48. Napper, R.M. and R.J. Harvey, *Quantitative study of the Purkinje cell dendritic spines in*
884 *the rat cerebellum.* J Comp Neurol, 1988. **274**(2): p. 158-67.
885 49. Isope, P. and B. Barbour, *Properties of unitary granule cell-->Purkinje cell synapses in*
886 *adult rat cerebellar slices.* J Neurosci, 2002. **22**(22): p. 9668-78.
887 50. Ekerot, C.F. and H. Jörntell, *Parallel fibre receptive fields of Purkinje cells and*
888 *interneurons are climbing fibre-specific.* Eur J Neurosci, 2001. **13**(7): p. 1303-10.
889 51. Dugué, G.P., et al., *Cerebellar re-encoding of self-generated head movements.* Elife,
890 2017. **6**.
891 52. Chen, S., G.J. Augustine, and P. Chadderton, *The cerebellum linearly encodes whisker*
892 *position during voluntary movement.* eLife, 2016. **5**: p. e10509-e10509.
893 53. Herzfeld, D.J., et al., *Encoding of action by the Purkinje cells of the cerebellum.* Nature,
894 2015. **526**(7573): p. 439-42.
895 54. Hong, S., et al., *Multiplexed coding by cerebellar Purkinje neurons.* Elife, 2016. **5**.
896 55. Apps, R. and M. Garwicz, *Anatomical and physiological foundations of cerebellar*
897 *information processing.* Nat Rev Neurosci, 2005. **6**(4): p. 297-311.
898 56. Apps, R. and R. Hawkes, *Cerebellar cortical organization: a one-map hypothesis.* Nat
899 Rev Neurosci, 2009. **10**(9): p. 670-81.

57. Ji, Z. and R. Hawkes, *Topography of purkinje cell compartments and mossy fiber terminal fields in lobules ii and iii of the rat cerebellar cortex: Spinocerebellar and cuneocerebellar projections.* Neuroscience, 1994. **61**(4): p. 935-954.
58. Larsell, O., *The Comparative Anatomy and Histology of the Cerebellum from Myxinoids through Birds*. 1967: The University of Minnesota Press.
59. Larsell, O., *The Comparative Anatomy and Histology of the Cerebellum from Monotremes through Apes*. 1970: The University of Minnesota Press, Minneapolis.
60. Mugnaini, E., *The length of cerebellar parallel fibers in chicken and rhesus monkey.* J Comp Neurol, 1983. **220**(1): p. 7-15.
61. Brand, S., A.L. Dahl, and E. Mugnaini, *The length of parallel fibers in the cat cerebellar cortex. An experimental light and electron microscopic study.* Exp Brain Res, 1976. **26**(1): p. 39-58.
62. Hámori, J., *Anatomy and neurochemical anatomy of the cerebellum*, in *Cerebellar degenerations : clinical neurobiology*, A. Plaitakis, Editor. 1992, Kluwer Academic.
63. Palay, S.L. and V. Chan-Palay, *Cerebellar cortex : cytology and organization*. 1974, Berlin: Springer.
64. Lange, W., *Regional differences in the distribution of golgi cells in the cerebellar cortex of man and some other mammals.* Cell Tissue Res, 1974. **153**(2): p. 219-26.
65. Barmack, N.H. and V. Yakhnitsa, *Functions of interneurons in mouse cerebellum.* J Neurosci, 2008. **28**(5): p. 1140-52.
66. Hámori, J. and J. Szentágothai, *Participation of Golgi neuron processes in the cerebellar glomeruli: an electron microscope study.* Exp Brain Res, 1966. **2**(1): p. 35-48.
67. D'Angelo, E., et al., *The cerebellar Golgi cell and spatiotemporal organization of granular layer activity.* Front Neural Circuits, 2013. **7**: p. 93.
68. Miles, F.A., et al., *Long-term adaptive changes in primate vestibuloocular reflex. III. Electrophysiological observations in flocculus of normal monkeys.* J Neurophysiol, 1980. **43**(5): p. 1437-76.
69. Edgley, S.A. and M. Lidierth, *The discharges of cerebellar Golgi cells during locomotion in the cat.* J Physiol, 1987. **392**: p. 315-32.
70. Galliano, E., P. Mazzarello, and E. D'Angelo, *Discovery and rediscoveries of Golgi cells.* J Physiol, 2010. **588**(Pt 19): p. 3639-55.
71. Eccles, J.C., R. Llinás, and K. Sasaki, *Golgi cell inhibition in the cerebellar cortex.* Nature, 1964. **204**: p. 1265-6.
72. Holtzman, T., et al., *Different responses of rat cerebellar Purkinje cells and Golgi cells evoked by widespread convergent sensory inputs.* J Physiol, 2006. **574**(Pt 2): p. 491-507.
73. Vos, B.P., A. Volny-Luraghi, and E. De Schutter, *Cerebellar Golgi cells in the rat: receptive fields and timing of responses to facial stimulation.* Eur J Neurosci, 1999. **11**(8): p. 2621-34.
74. Hartmann, M.J. and J.M. Bower, *Tactile responses in the granule cell layer of cerebellar folium crus IIa of freely behaving rats.* J Neurosci, 2001. **21**(10): p. 3549-63.
75. Arenz, A., et al., *The contribution of single synapses to sensory representation in vivo.* Science, 2008. **321**(5891): p. 977-80.
76. van Kan, P.L., A.R. Gibson, and J.C. Houk, *Movement-related inputs to intermediate cerebellum of the monkey.* J Neurophysiol, 1993. **69**(1): p. 74-94.

945 77. Giovannucci, A., et al., *Cerebellar granule cells acquire a widespread predictive*
946 *feedback signal during motor learning.* Nat Neurosci, 2017.
947 78. Pietrajtis, K. and S. Dieudonné, *Golgi Neurons*, in *Handbook of the Cerebellum and*
948 *Cerebellar Disorders*, M. Manto, et al., Editors. 2013, Springer Netherlands: Dordrecht.
949 p. 829-852.
950 79. Eyre, M.D. and Z. Nusser, *Only a Minority of the Inhibitory Inputs to Cerebellar Golgi*
951 *Cells Originates from Local GABAergic Cells.* eNeuro, 2016. **3**(2).
952 80. Dumoulin, A., A. Triller, and S. Dieudonné, *IPSC kinetics at identified GABAergic and*
953 *mixed GABAergic and glycinergic synapses onto cerebellar Golgi cells.* J Neurosci, 2001.
954 **21**(16): p. 6045-57.
955 81. Hull, C. and W.G. Regehr, *Identification of an inhibitory circuit that regulates cerebellar*
956 *Golgi cell activity.* Neuron, 2012. **73**(1): p. 149-58.
957 82. Vervaeke, K., et al., *Rapid desynchronization of an electrically coupled interneuron*
958 *network with sparse excitatory synaptic input.* Neuron, 2010. **67**(3): p. 435-51.
959 83. Ruigrok, T.J., R.A. Hensbroek, and J.I. Simpson, *Spontaneous activity signatures of*
960 *morphologically identified interneurons in the vestibulocerebellum.* J Neurosci, 2011.
961 **31**(2): p. 712-24.
962 84. Rossi, D.J., M. Hamann, and D. Attwell, *Multiple modes of GABAergic inhibition of rat*
963 *cerebellar granule cells.* J Physiol, 2003. **548**(Pt 1): p. 97-110.
964 85. Mapelli, L., S. Solinas, and E. D'Angelo, *Integration and regulation of glomerular*
965 *inhibition in the cerebellar granular layer circuit.* Front Cell Neurosci, 2014. **8**: p. 55.
966 86. Ros, H., et al., *Neocortical networks entrain neuronal circuits in cerebellar cortex.* J
967 Neurosci, 2009. **29**(33): p. 10309-20.
968 87. Rasmussen, A., et al., *Golgi cell activity during eyeblink conditioning in decerebrate*
969 *ferrets.* Cerebellum, 2014. **13**(1): p. 42-5.
970 88. DiGregorio, D.A., et al., *Desensitization properties of AMPA receptors at the cerebellar*
971 *mossy fiber granule cell synapse.* J Neurosci, 2007. **27**(31): p. 8344-57.
972 89. DiGregorio, D.A., Z. Nusser, and R.A. Silver, *Spillover of glutamate onto synaptic AMPA*
973 *receptors enhances fast transmission at a cerebellar synapse.* Neuron, 2002. **35**(3): p.
974 521-33.
975 90. Chabrol, F.P., et al., *Synaptic diversity enables temporal coding of coincident*
976 *multisensory inputs in single neurons.* Nat Neurosci, 2015. **18**(5): p. 718-27.
977 91. Sherman, S.M. and R.W. Guillery, *Distinct functions for direct and transthalamic*
978 *corticocortical connections.* J Neurophysiol, 2011. **106**(3): p. 1068-77.

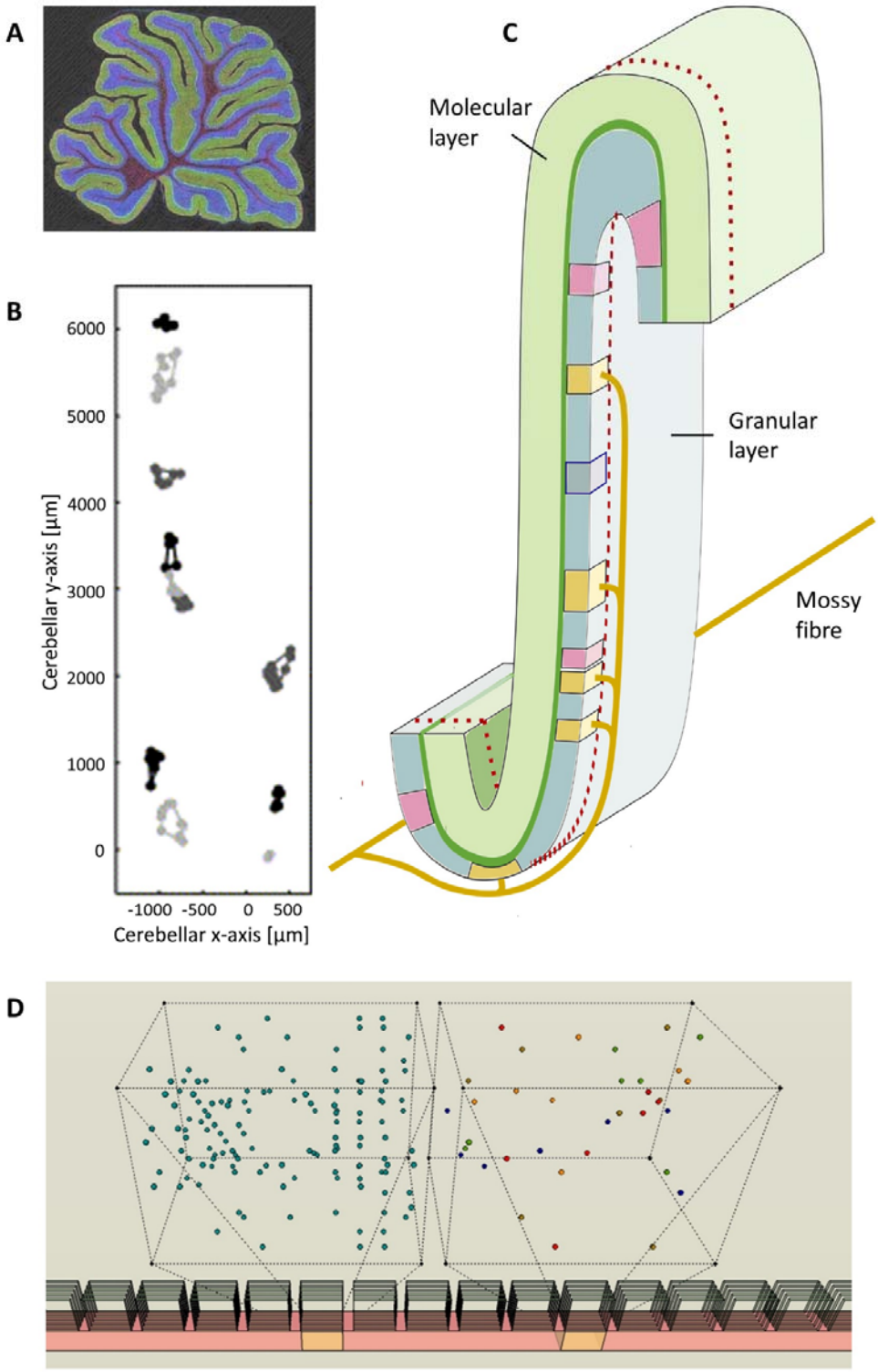
A
B
C
D
Molecular layer
Granular layer
Mossy fibre
Cerebellar y-axis [µm]
Cerebellar x-axis [µm]
6000
5000
4000
3000
2000
1000
0
-1000
-500
0
500

979

980 **Fig 1. Mossy fibre termination. A** Sagittal section of the rat cerebellum (obtained by
981 multi-photon microscopy, courtesy Tom Deerinck). The outer layer of the cerebellar
982 cortex, the molecular layer, is stained green and the inner layer, the granular layer, is
983 blue. **B** Output of a procedure used to group mossy fibre terminals into clusters [20 fig
984 6], reproduced with permission. All terminals belong to one mossy fibre, which
985 terminates in two strips. Clusters are shown in different shades of grey. **C** Schematic of
986 an area of the folded cerebellar cortex. The strip inside the red dotted line is the width
987 and depth of a microzone but only part of its length. Termination of mossy fibre signals
988 is not at a point but at several randomly spaced, sagittally-aligned locations. Yellow
989 zones are terminal locations of a single mossy fibre. Size of locations varies depending
990 partly on the number of terminals in each cluster. Pink zones are terminal locations of
991 a second mossy fibre. In reality, zones overlap extensively and terminals are
992 intermingled. A mossy fibre mediolateral axon may give rise to several sagittal
993 branches, of which here only one is shown. The zone enclosed by a blue line has the
994 dimensions of a 'field'. A field is a nominal division of the granular layer with the
995 average dimensions of a mossy fibre terminal cluster – 200 µm x 150 µm – which we
996 use to quantify granular layer computations. A strip of the granular layer with the
997 dimensions of a sagittal row of 75–100 fields is a 'rank'. Viewed from the cerebellar
998 surface, a rank has the dimensions of a mid-range estimate of a microzone, but its long
999 sides are less cleanly defined. **D** Section of a microzone viewed obliquely from the
1000 cerebellar surface, to illustrate the size and random intermingling of mossy fibre
1001 terminals. The molecular layer is represented by squares of about the dimensions of a
1002 Purkinje cell territory. The wire frame boxes are an exploded view of the orange fields.
1003 The right box shows randomly distributed terminals of 5 mossy fibres (each a different
1004 colour). We estimate that ~180 mossy fibres contribute terminals to a field, and a field
1005 contains a total of around 700 terminals. Proportions of terminal size to field size are
1006 preserved. The left box shows terminals of 20 mossy fibres.

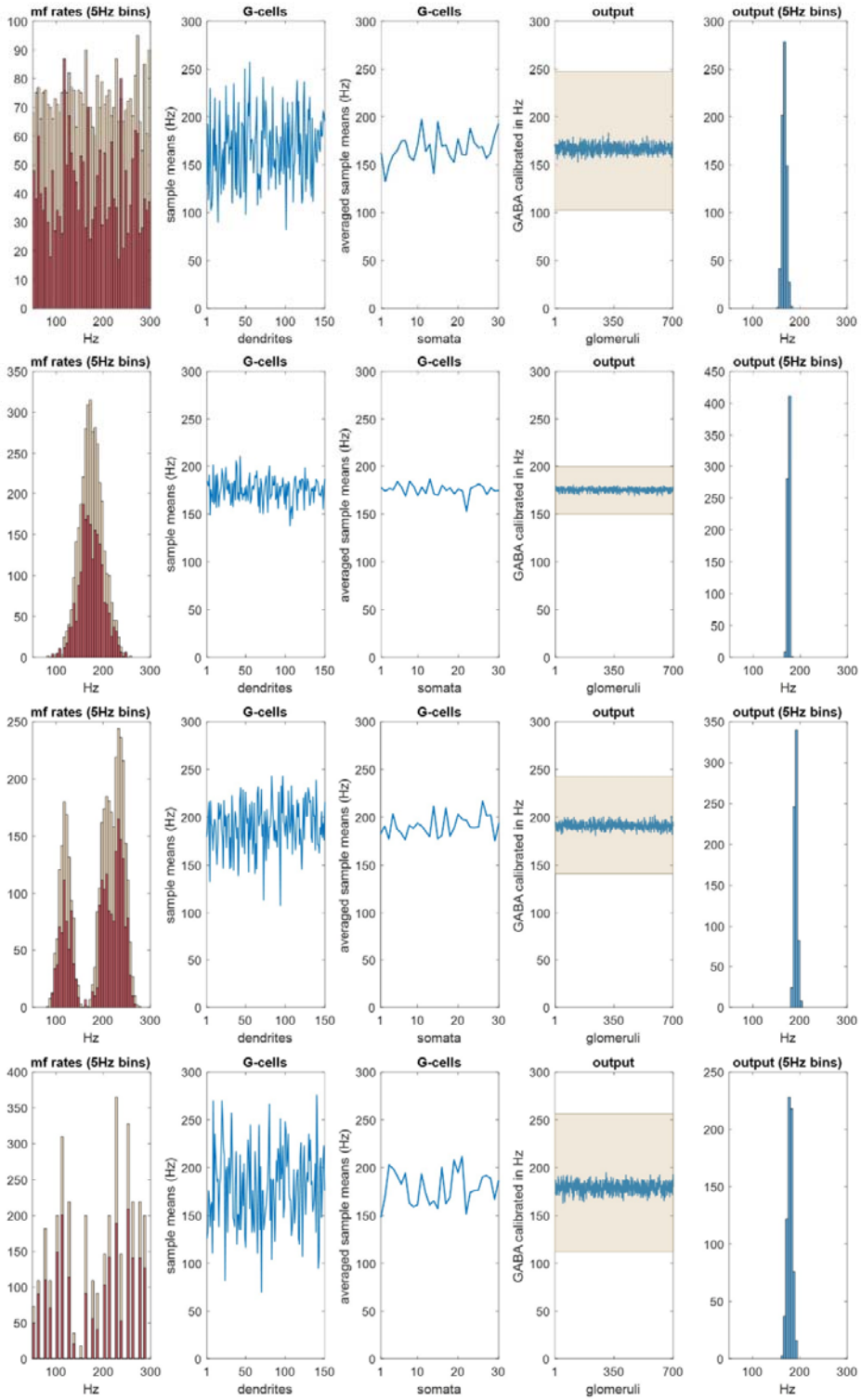
mf rates (5Hz bins)
G-cells
G-cells
output
output (5Hz bins)
Hz
dendrites
somata
glomeruli
Hz
sample means (Hz)
averaged sample means (Hz)
GABA calibrated in Hz

1007

1008 **Fig 2. Golgi cell ensemble conversion. Column 1** We randomly generated (3,645)
1009 values representing mossy fibre rates with a uniform, normal, twin-peaked or
1010 discontinuous distribution, simulating input to a row of 100 fields. Rate data were
1011 randomly sampled to derive input rates to each field, and copies added to reflect the
1012 fact that each afferent cell contributes a randomly variable number of terminals. Red
1013 data represent copies-included signals received by a row of three fields. See Methods
1014 for derivation of rates. **Column 2** The first-column red data were randomly sampled
1015 150 times, sample size 4, representing mossy fibre input to a 3-field population of 30
1016 Golgi cells, each with 5 basal dendrites (the mean) which each receive contact from 4
1017 mossy fibres. Data are the sample means, representing dendritic depolarisation.
1018 **Column 3** We next randomly sampled column 2 data *without* replacement 30 times,
1019 sample size 5, and took the sample means, representing somatic integration of
1020 dendritic signals. **Column 4** Column 3 data were randomly sampled 700 times, sample
1021 size 8–12, reflecting convergent input from 3 fields of Golgi cells onto 700 glomeruli in
1022 the middle field (which receives the output of a three-field ensemble), and took the
1023 sample means, representing GABA spillover that is a linear function of the mean of
1024 afferent rates. Inhibition of granule cells is almost exclusively mediated by spillover.
1025 **Column 5** The column 4 data are presented as a histogram. **All rows** Column 1 mossy
1026 fibre data are converted to narrowly-focussed inhibition of granule cells. The mean of
1027 the column 4/5 data is linearly related to the mean of the mossy fibre distribution. This
1028 result is independent of the shape of the original distribution.

1029

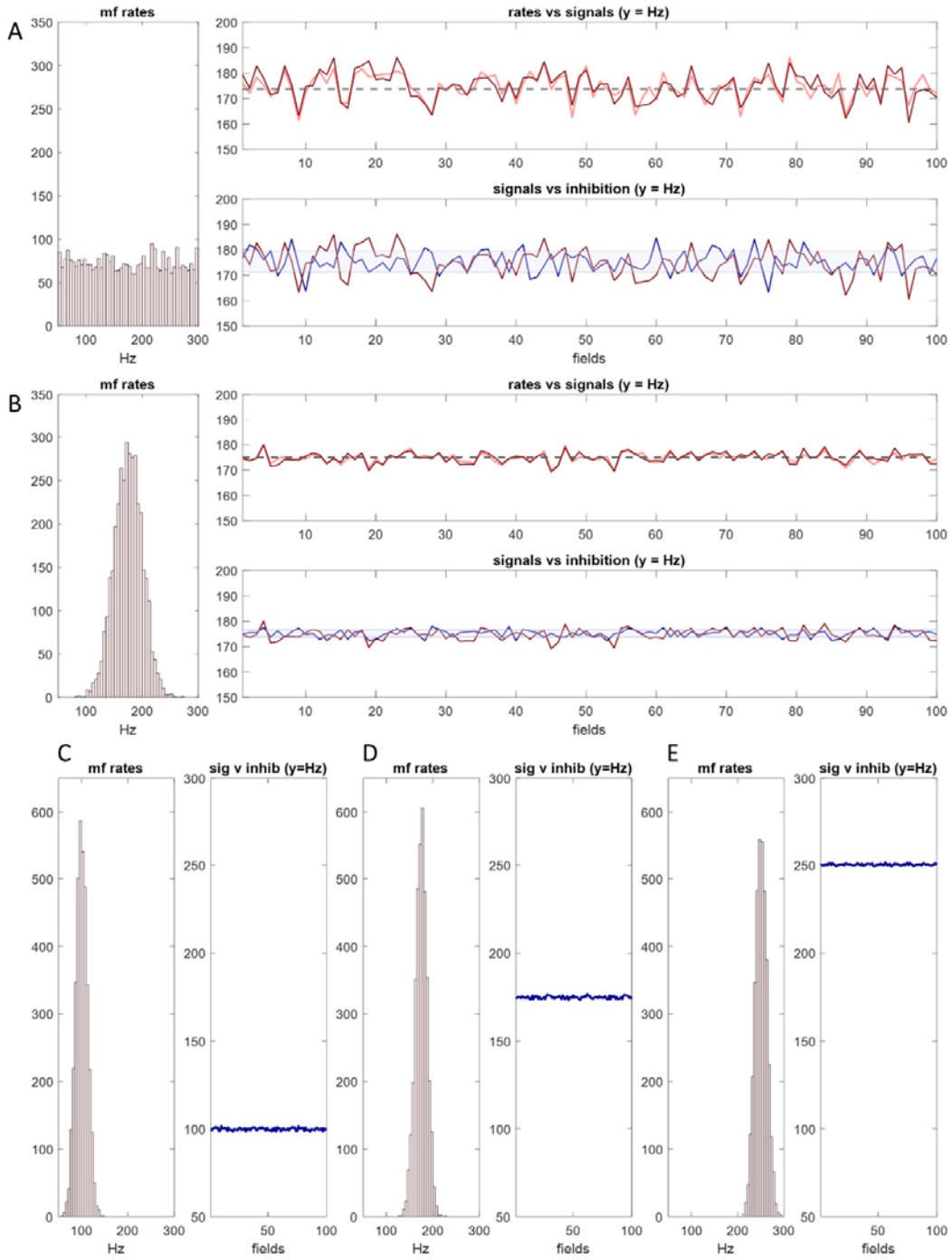
A
mf rates
Hz
rates vs signals (y = Hz)
signals vs inhibition (y = Hz)
fields
B
mf rates
Hz
rates vs signals (y = Hz)
signals vs inhibition (y = Hz)
fields
C
mf rates
Hz
sig v inhib (y=Hz)
fields
D
mf rates
Hz
sig v inhib (y=Hz)
fields
E
mf rates
Hz
sig v inhib (y=Hz)
fields

1032 **Fig 3. The Golgi cell population of a rank functions as a single unit. A** Simulation of
1033 Golgi cells in a sagittal row of 100 fields, taking the mossy fibre distribution on the left
1034 as input (see Fig 2 and Methods for derivation of mossy fibre rates). **Top right**: pink:
1035 the mean of mossy fibre input rates to each field; red: the mean with duplicate signals
1036 added; dashed grey line: the mean of input rates to the whole rank. **Bottom right**: red:
1037 same as top right; blue: mean, for each field, of glomerulus data derived in the same
1038 way as Figure 2 columns 4 and 5 (the 'inhibitory field mean'); pale blue: SD of
1039 glomerulus data. **B** Same as (A) but sampling a different mossy fibre distribution.

1040 **A and B**

1041 Red data closely track the pink data in top right panels, indicating that duplicate signals
1042 (because the mossy fibre axon ends in a cluster of terminals) do not skew the mean of
1043 firing rates received by a field.

1044 Blue data across all fields are in a narrowly circumscribed range. Focus varies with the
1045 bandwidth of the sampled distribution (mossy fibre rates). A normal mossy fibre
1046 distribution with a range of over 100 Hz is converted to a blue range of ~3 Hz.

1047 Inhibitory field means are tightly grouped: inhibition of granule cells is synchronised in
1048 a rank.

1049 The range of the blue data is centred on the grey dashed line – the mean of mossy
1050 fibre input rates received by the whole rank – and varies independently of the red
1051 data. That is, unpredictability inherent in the mechanism (because the outcome of
1052 random sampling is inherently uncertain) is not compounded; random variation of the
1053 red data doesn't flow through to amplify random variation of the blue data (in fact the
1054 blue data have a slightly smaller range).

1055 **C** The same simulation. Left: the sampled distribution (mossy fibre input rates to a
1056 rank); right: the inhibitory field means (we use the means to compare fields). The y axis
1057 of the right panel has the same range as the x axis of the left panel. Panels are tall to

1058 improve visual comparison to other rows, where the y axis has a smaller range. **D** and **E**
1059 The same, moving the sampled distribution to the right. Inhibition of granule cells is
1060 precisely and linearly coupled to the mean of mossy fibre input rates to the whole
1061 rank.

1062

1063

1064

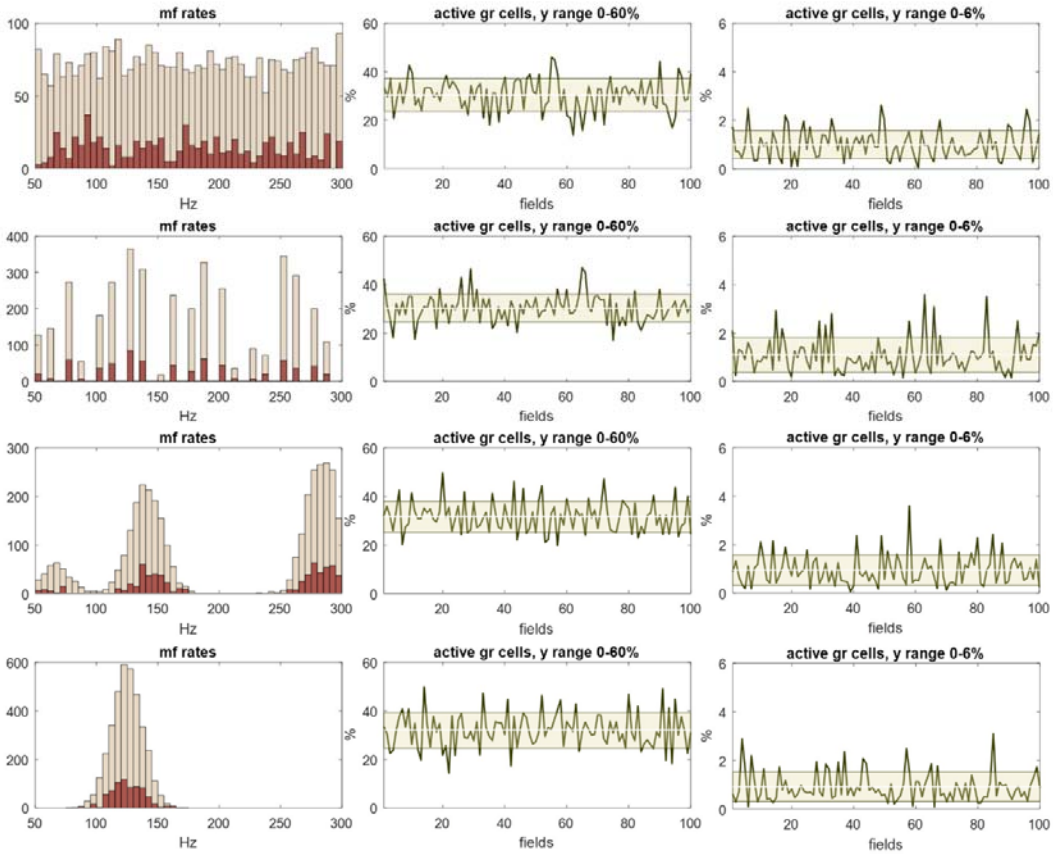

1065

1066

1067 **Fig 4. Regulation of granule cell activity by the feed-forward pathway (mossy**
1068 **fibres→Golgi cells→granule cells)** We incorporated the Golgi cell ensemble
1069 conversion into a simulation of the conversion of mossy fibre signals into granule cell

1070 signals (recoding). One of the outputs of recoding is regulation of the percentage of
1071 active granule cells. We tested if the recoding computation causes the percentage to
1072 be stable, i.e., in the same narrow range in all fields regardless of the distribution of
1073 mossy fibre rates. **Column 1** Mossy fibre firing rates were randomly generated with a
1074 uniform, discontinuous, three-peak or normal distribution, to represent input to a row
1075 of 100 fields. Rates, and rates received by each field, were derived in the same way as
1076 earlier Figures. Red data are rates received by a single randomly-selected field,
1077 including duplicate signals. y axes are scaled to the data – all distributions contain the
1078 same number of signals. **Column 2** The percentage of granule cells that fire in each
1079 field. The Golgi cell computation includes no adjustment to sparsen granule cell
1080 activity. The white line and shaded area are mean and SD. **Column 3** The same, with an
1081 adjustment (a co-efficient) to sparsen granule cell activity. y axes have 1/10 the range
1082 of column 2. The percentage is confined to a narrow range. This result is independent
1083 of the sampled (i.e., mossy fibre) distribution, suggesting that regulation is
1084 independent of fluctuation of mossy fibre rates. Nonetheless, field-to-field variation
1085 relative to the mean is significant. Homeostatic local fine tuning may be provided
1086 physiologically by feedback via granule cell ascending axon contact on Golgi cells, not
1087 represented in the simulation.

1088

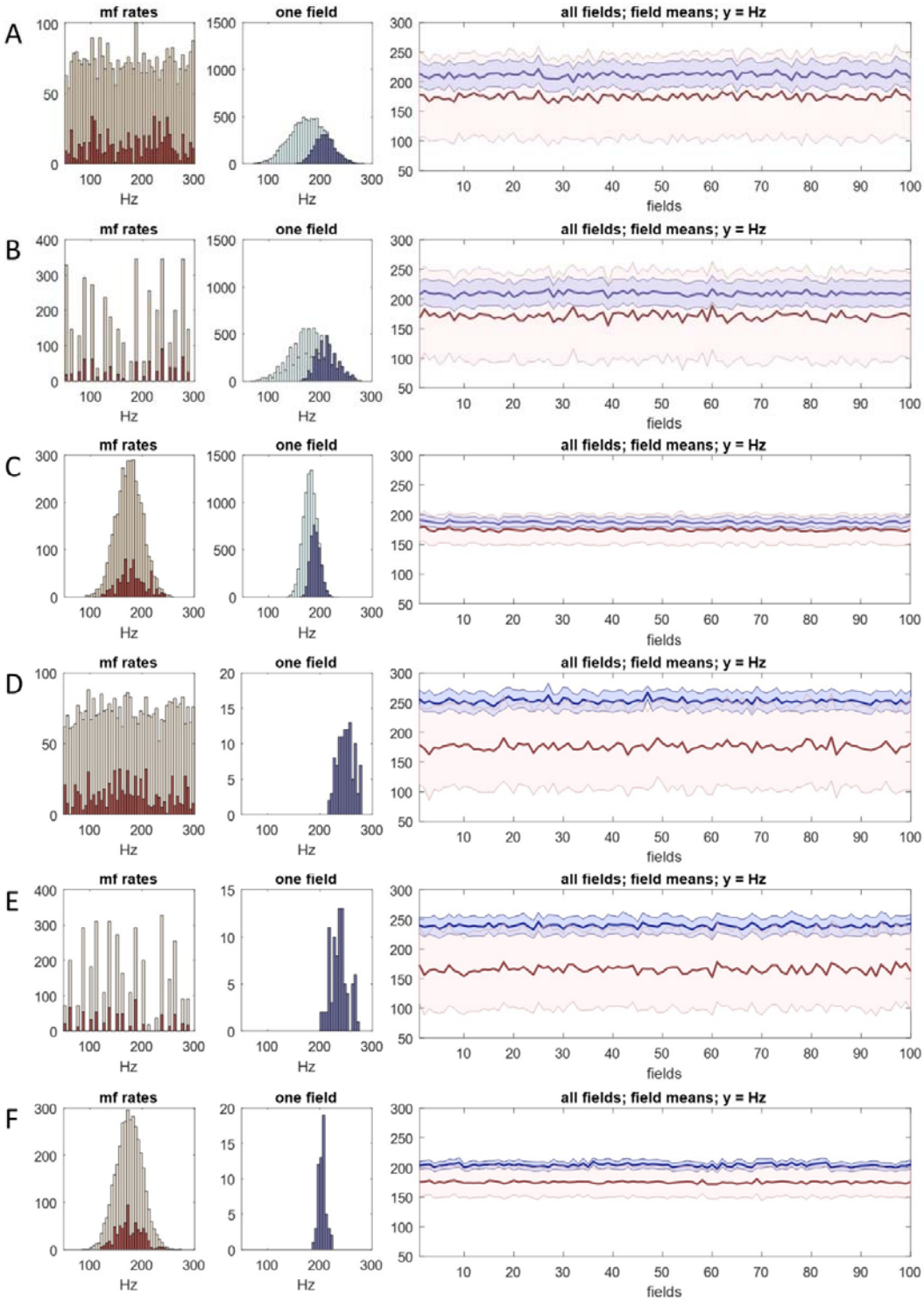
A
B
C
D
E
F
mf rates
one field
all fields; field means; y = Hz
Hz
fields

1089

1090 **Fig 5. A rank is a single recoding unit.** The same simulation as Figure 4 but data are
1091 granule cell firing rates or derived from granule cell firing rates. **Column 1** We tested
1092 the effect of changing the shape of the mossy fibre distribution (without changing the
1093 number of signals). **Column 2** Pale green: sample means – the mean of input rates to
1094 each granule cell in a single field selected at random; blue: sample means of the subset
1095 of granule cells which meet the conditions to fire. In rows A–C, ~30% fire. In rows D–F,
1096 ~1% fire, y axes are rescaled and green data are omitted. **Column 3** Red: mean of
1097 mossy fibre input rates to each field in a rank, including duplicate signals; pink: SD of
1098 mossy fibre input rates to each field; blue: field means (i.e., the mean of granule cell
1099 firing rates in each field); pale blue: SD of granule cell firing rates in each field.

1100 **Observations**

1101 Regardless of the shape and large range of the mossy fibre distribution, the field
1102 means always converge towards a straight line which is a fixed distance from the
1103 overall mean of mossy fibre rates.

1104 The amount and direction of field-to-field random fluctuation of the blue data is
1105 independent of local fluctuation of the red data, and in a smaller range. Uncertainty
1106 inherent in random sampling – first by single fields of input rates to a rank, and then by
1107 Golgi cells and granule cells of input rates to a field – is not compounded.

1108

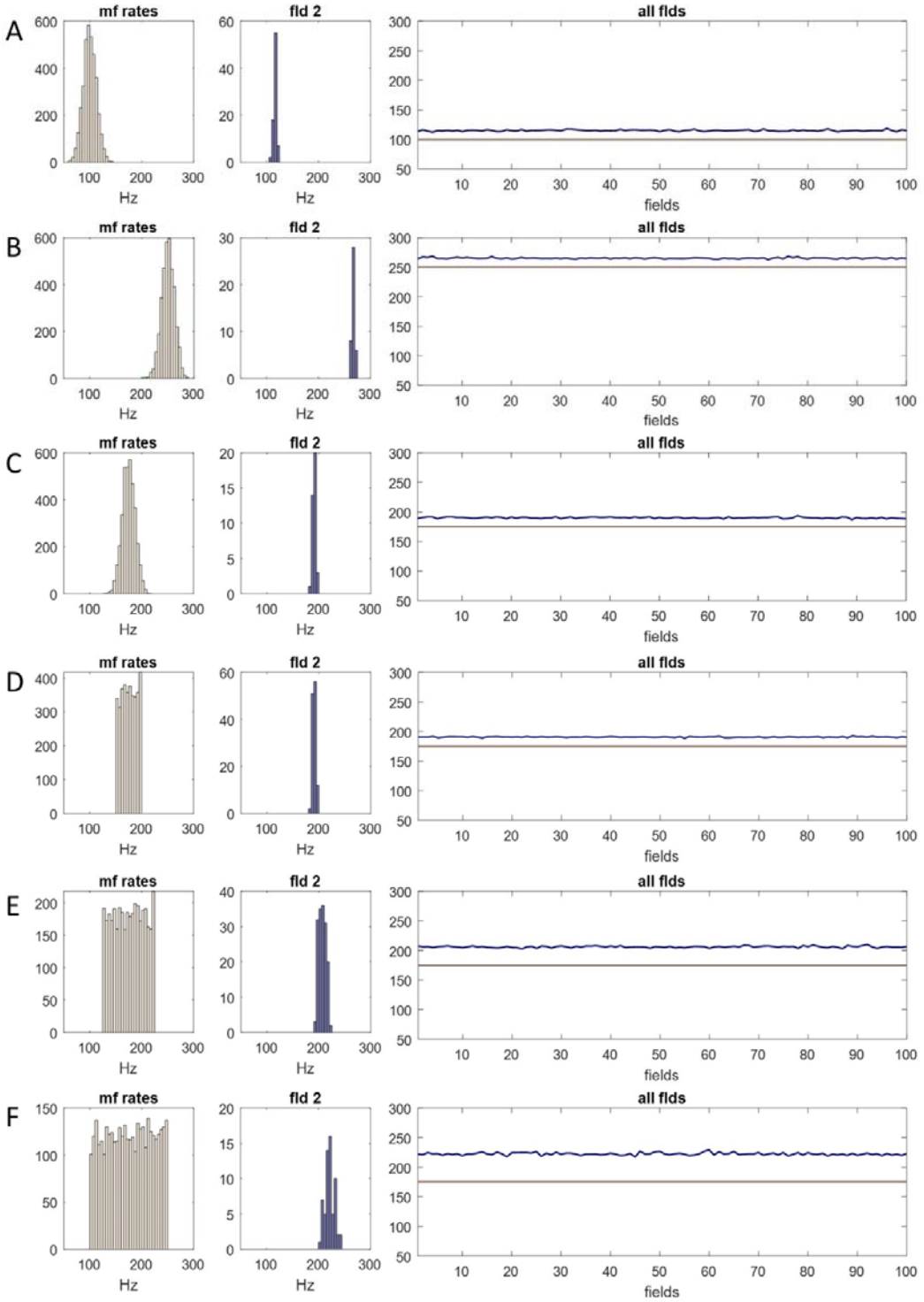

1109

1110 **Fig 6. Granule cells collectively code mossy fibre rate information. Column 1** Mossy
1111 fibre rates were generated in the same way as earlier Figures, with either a normal (SD
1112 12.5) or uniform distribution representing input to a row of 100 fields, with copies
1113 added – the sampled distribution. **Column 2** Histogram of granule cell firing rates in a
1114 randomly selected field, obtained in the same way as in the bottom 3 rows of Fig 5.
1115 **Column 3** Grey line: the mean of the sampled distribution; blue line: field means. **A–C**
1116 The fields means are precisely and linearly related to the mean of mossy fibre rates.
1117 Blue data approach a straight line which is parallel to the grey line at a mean distance
1118 of 15 Hz (SD 1.21 Hz). **D–F** If the shape and mean of a uniform sampled distribution are
1119 unchanging, the distance between the blue and grey lines is linearly related to the
1120 range.

1121